Analysis of heavy ion beam probe potential measurement errors in the Madison Symmetric Torus

X. Zhang, J. Lei, K. A. Connor,[a] D. R. Demers, P. M. Schoch, and U. Shah
Rensselaer Polytechnic Institute, Troy, New York 12180

The heavy ion beam probe on the Madison Symmetric Torus is capable of measuring the plasma potential at radial locations from about $\rho = r/a = 0.3$ to 0.75. Radial potential scans from two energy analyzer detectors have been used to assess measurement accuracy since they should produce identical profiles. The effects of analyzer characteristics, system alignment, sample volume locations and shapes, probing beam control, the quality of confining magnetic field information available, etc., have been assessed to determine the overall quality of the potential measurements. The accuracy of the measurements is found to be quite good relative to the potentials measured. © *2004 American Institute of Physics.* [DOI: 10.1063/1.1787953]

The heavy ion beam probe (HIBP)[1] has measured the local electric potential on the Madison Symmetric Torus (MST). MST[2] is a reversed field pinch with major radius $R = 1.5$ m, minor radius $a = 0.52$ m, toroidal plasma current $I_\varphi \leq 500$ kA, and beta $\beta \leq 15\%$. The data considered in this article were acquired in standard (low confinement) plasma discharges with a plasma current of 355–380 kA and a density of $0.65 \times 10^{13} – 1.15 \times 10^{13}/\text{cm}^3$. The plasma potential, measured in the core with an HIBP, ranges from 0.5 to 2.5 kV[3,4] for such discharges. However, the scatter in the data is quite large, which can make it difficult to obtain accurate potential and electric field profiles. This article considers instrumental sources of error, as opposed to variations in plasma conditions, which may contribute to potential variations, and their impact on the quality of the equilibrium potential profile measurements. In Sec. I, the HIBP potential measurement principle is introduced and the results of equilibrium potential profile measurements are presented. In Sec. II the effects of calibration factors, magnetic equilibrium reconstruction, and scrape-off on the accuracy of potential profiles measurement are addressed. Results are summarized in Sec. III.

I. INTRODUCTION AND POTENTIAL MEASUREMENT RESULTS

The MST-HIBP has used singly charged Na and K probing ions with energies ranging from 40 to 70 keV. The probing ions are further ionized in the confining magnetic field to doubly charged particles by impact with plasma electrons and then separated from the primaries by the increased Lorentz forces. Only those secondary ions originating from a limited ionization location (the sample volume) can reach the detector location, which allows for localized measurements in the plasma. The spatial resolution is determined by the size of the sample volumes, which varies from 0.3 to 3 cm for the conditions considered.

The MST-HIBP uses a Proca-Green-type 30° parallel plate electrostatic energy analyzer as a detector[4,5] (cf. Fig. 2 in Ref. 4). There are three detectors (top, center, and bottom), which correspond to three entrance apertures. Commonly, the HIBP obtains simultaneous measurements at three sample volumes. However, the MST-HIBP uses the top detector as a reference signal to remove the noise on the detectors generated by plasma UV radiation. Each detector is comprised of four plates referred to as upper, lower, left and right plates. The position of the secondary beam on the detector plates, along with the difference of the primary and secondary beam energies,[4] is used to compute the plasma potential

$$\phi = 2V_a \left\{ G(\theta_I, \alpha) + F(\theta_I, \alpha) \frac{i_U - i_L}{i_U + i_L} \right\} - V_g. \quad (1)$$

The variables V_a and V_g are the analyzer and accelerating voltage, respectively; i_U and i_L are the currents on the two upper and two lower detector plates; θ_I is the entrance angle of the beam into the detector; and α is the out of plane angle. The gain function, G, and off-line processing function, F, will be discussed in Sec. II.

During a standard discharge, a 70 keV Na$^+$ beam is injected into the plasma and steered with electrostatic sweep plates to radial locations from $0.3 < r/a < 0.75$. Signals are acquired throughout the discharges. Windows (0.5 ms) of data at times between sawtooth crashes are selected for which the total detected signal exceeds 20 nA.[6,7] Figure 1 shows the potential profiles measured by the center (φ_c) and bottom (φ_b) detectors obtained from 25 standard discharge shots. Each point represents the ensemble average potential at the positions indicated. The data are fitted with a quadratic line using the least-square method (solid line). The region of measurement was then uniformly divided and the ensemble averaged data points from each region were used to compute a local average potential and standard deviation; these are shown as the straight lines, with error bars, in Fig. 2. The fitted potential lines are also re-plotted for clarity in Fig. 2. The differences in the two potential profiles are smaller than
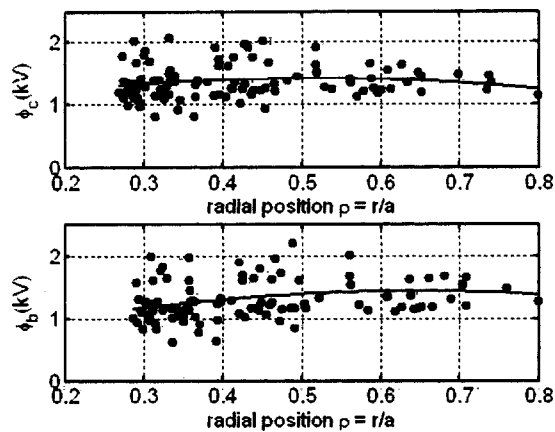
---

[a]Author to whom correspondence should be addressed; electronic mail: connor@rpi.edu

FIG. 1. Equilibrium potential profile on the center detector plate φ_c (top plot) and the bottom detector plate φ_b (bottom plot).

the scatter in the data. Thus, the primary conclusion is that the two profiles are essentially the same; a typical MST potential profile is quite flat and the radial electric field is small. However, the differences in the two profiles consistently appear in all experiments. Thus, the systematic differences in the profiles have been investigated to determine if they are caused by instrumental errors. Profiles with improved accuracy result from this exercise.

II. ANALYSIS OF POTENTIAL PROFILE MEASUREMENT ACCURACY

Systematic differences between what should be identical measurements can be used to identify and possibly correct for sources of error. Possible sources of instrumental errors were investigated to determine if the potential profiles of both detectors φ_c and φ_b could be made more alike.

A. Gain function *G* and off-line processing function *F*

The two functions used to characterize an HIBP analyzer are the gain function $G(\theta_I, \alpha)$ and off-line processing function $F(\theta_I, \alpha)$. Unlike most HIBP systems, *in situ* calibration is not possible on MST. Hence the system was reconfigured so that a primary ion beam was directed to the analyzer through the secondary beam line.[8] The calibration addressed only variations of G and F as a function of the in-plane
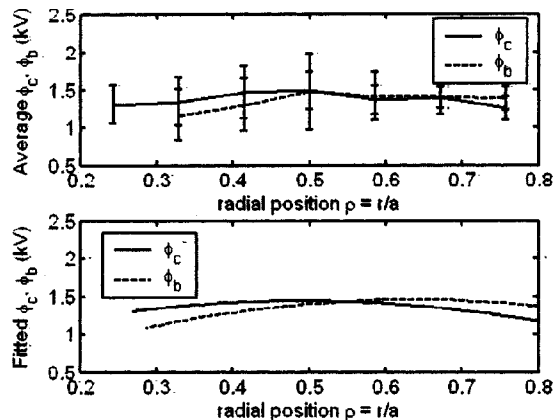
TABLE I. Gain, F and θ_I effect on potential φ (assuming $V_a = 12$ kV)

	Max	Min	$\Delta = \text{max} - \text{min}$	$\Delta\varphi$(kV)
G	2.9767	2.9708	0.0059	0.142
F	0.0477	0.0345	0.0123	0.507

entrance angle θ_I since the out-of-plane angle α is within $\pm 0.5°$ mostly due to the limitations of the secondary beam alignment.[7] Thus, the effect of α on G and F, proportional to $\cos^2(\alpha)$,[4] is negligible ($<0.03\%$).

G and F terms were calibrated with a 2 mm entrance slit width and the data were fitted to Eqs. (7) and (8) of Ref. 4 by adjusting the geometric parameters of the analyzer (X_D and Y_D) with θ_I ranging from 22.5° to 37°. Exceptionally good agreement between the calibration and simulation data obtained for both the bottom and center detectors (error is less than 3×10^{-4}) was obtained with $X_D = 654.03$ mm and $Y_D = 124.96$ mm. There is no direct measure of analyzer entrance angle in an HIBP measurement. Rather, θ_I is obtained from the trajectory simulation program which uses the magnetic field generated by the toroidal equilibrium code MSTFit.[9] Scanning the ion beam from $\rho = 0.3$ to 0.75, θ_I is found to be in the range $30 \pm 3°$[10,11] (center: 28.5°–33°; bottom 27.3°–32°) with θ_I increasing with radius. The maximum variation of G and F (shown in Table I) can result in errors up to 10% and 30% (the average potential is assumed to be 1.5 kV). This demonstrates that G, F and θ_I must all be known well.

θ_I is never precisely known due to uncertainties in the trajectory simulation program and/or inaccurate measurements of the position and the orientation of the HIBP energy analyzer. To determine whether the entrance angles are off by some fixed amount, the G and F curves were shifted by up to $\pm 3°$ to simulate this effect. The best agreement between the two potential profiles φ_c and φ_b was obtained by right-shifting θ_I 2°, as shown in Fig. 3. Observe that the two profiles now appear to be essentially the same, except for a shift in position. This suggests that the remaining differences may be due to inaccurate determination of the sample locations.
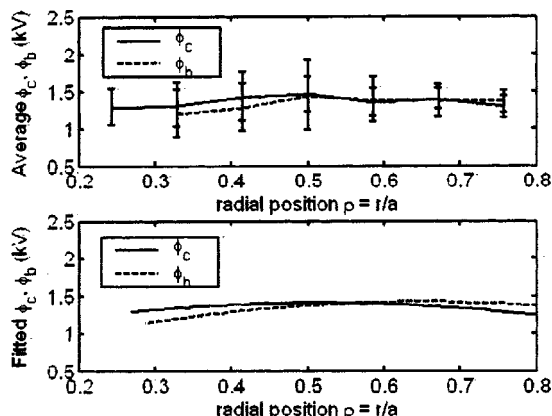

FIG. 2. Locally averaged potential profile with error bars (top plot) and fitted potential profiles (bottom plot) for φ_c and φ_b from Fig. 1.

FIG. 3. Averaged potential profile with error bars (top plot) and fitted potential profiles (bottom plot) for φ_c and φ_b when θ_I is right-shifted 2° (original potential profiles are shown as Fig. 2).
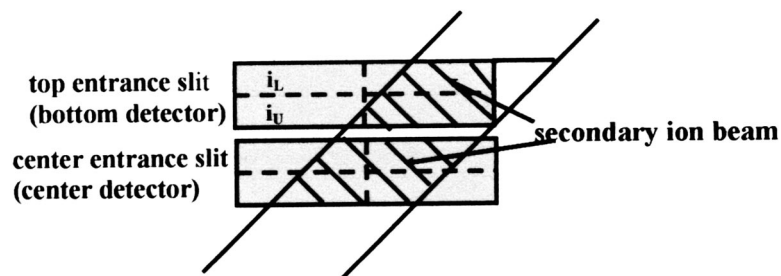
FIG. 4. Schematic of secondary beam scrape-off when $r/a > 0.55$.

B. Sensitivity of sample volume position with equilibrium magnetic field

The location of the HIBP sample volume and secondary entrance angle θ_I during a plasma discharge is computed with a trajectory simulation code, which utilizes magnetic field equilibria generated by the equilibrium modeling code MSTFit.[9] Equilibria generated correspond to one point in time during a plasma discharge; equilibria in MST can vary a great deal during a discharge and from shot to shot. We do not generate magnetic equilibria for multiple shots and multiple time windows; instead one field with an average plasma current of 363 kA is used to compute the sample volume location of all data points for the potential profiles in Figs. 1 and 2. To determine the sensitivity to variations in magnetic field, the sample volume locations were computed using two additional magnetic equilibria corresponding to plasma currents of 370 and 375 kA (increasing plasma current moves the sample volumes inward, but not necessarily monotonically). Near $\rho \cong 0.33$, the change is smaller (3–4 cm) than near $\rho \cong 0.75$ (5–7 cm). Such changes could account for much of the remaining differences in the two potential profiles. However, the sample locations do not change systematically with magnetic configuration so there is no simple way to use this information to improve the profile. Also, note that the entrance angle θ_I will also change, but only by at most 0.5° for the three equilibria.

C. Signal scrape-off effect

The effect on the detected ion signal due to mechanical interference with the beam in the secondary beam line, entrance and exit ports, and entrance slit apertures, is known as scrape-off. A schematic of the fan of secondary beam ions originating from the plasma and impinging upon the entrance apertures corresponding to the center and bottom detectors is shown in Fig. 4. The beam is slanted in the toroidal direction due to the nonuniform poloidal magnetic field. If the beam is well positioned relative to the center entrance aperture but poorly positioned relative to the top aperture (the usual case for the data shown here) and thus partially blocked by the aperture corresponding to the bottom detector, the detected ion current on the bottom detector will decrease. Recall that each detector consists of four plates. A loss of signal, due to scrape-off on the two upper-most plates shown in the figure

(corresponding to lower plate current i_L) will result in larger measured potential on the bottom detector φ_b. When the beam is scanned and the sample volumes are located near the core of the plasma, $r/a < 0.5$, most of the secondary beam will move to the left side of the entrance apertures and scrape-off effects will happen on both detectors. However, this will occur first on the bottom detector, which very likely accounts for most of the differences in the two profiles. Qualitatively, this change is observed on detected signals, but it is difficult to account for any changes in detail since the beam cannot be monitored at every location.

D. Obtaining improved measurements

Improved information on the potential for this and other operating conditions (especially improved confinement, where the potential is seen to be quite different) will require reduced data scatter. To realize this improvement, more intense probing beam current and improved beam control will be necessary. A fivefold increase of beam intensity has been obtained primarily through better modeling of the primary ion beam accelerator. Improved beam steering is being obtained by the application of a magnetic field in the vicinity of the secondary steering plates to mitigate the UV induced electron currents. A secondary beamline feedback system to obtain detected signal for a larger fraction of each discharge is also planned.

ACKNOWLEDGMENTS

[1] T. P. Crowley, IEEE Trans. Plasma Sci. **22**, 291 (1994).
[2] R. N. Dexter *et al.*, Fusion Technol. **19**, 131 (1991).
[3] K. A. Connor *et al.*, in *IEEE Conference Record-Abstracts. PPPS-2001 Pulsed Power Plasma Science 2001. 28th IEEE International Conference on Plasma Science and 13th IEEE International Pulsed Power Conference (Cat. No. 01CH37255); Piscataway, NJ* (IEEE, New York, 2001), p. 624.
[4] L. Solensten and K. A. Connor, Rev. Sci. Instrum. **58**, 516 (1987).
[5] T. S. Green and G. A. Proca, Rev. Sci. Instrum. **41**, 1409 (1970).
[6] J. Lei *et al.*, Phys. Rev. Lett. **89**, 275001/1 (2002).
[7] U. Shah, Ph.D thesis, Rensselaer Polytechnic Institute, 2001.
[8] J. Lei *et al.*, Rev. Sci. Instrum. **72**, 564 (2001).
[9] J. K. Anderson, Ph.D thesis, University of Wisconsin-Madison, 2001.
[10] J. Lei *et al.*, Rev. Sci. Instrum. **70**, 967 (1999).
[11] D. R. Demers *et al.*, Czech. J. Phys. **51**, 1065 (2001).